Renormalisation Group Analysis of Single Right-handed Neutrino Dominance

S. F. King and N. Nimai Singh [1]

Department of Physics and Astronomy, University of Southampton, Southampton,

SO17 1BJ, U.K.

Abstract

We perform a renormalisation group (RG) analysis of neutrino masses and mixing angles in the see-saw mechanism in the minimal supersymmetric standard model with three right-handed neutrinos, including the effects of the heavy neutrino thresholds. We focus on the case that one of the right-handed neutrinos provides the dominant contribution to the 23 block of the light Majorana matrix, causing its determinant to approximately vanish and giving an automatic neutrino mass hierarchy, so called single right-handed neutrino dominance which may arise from a $U(1)$ family symmetry. In these models radiative corrections can increase atmospheric and solar neutrino mixing by up to about 10% and 5%, respectively, and may help to achieve bi-maximal mixing. Significantly we find that the radiative corrections over the heavy neutrino threshold region are at least as important as those usually considered from the lightest right-handed neutrino down to low energies.

---

[1]On leave from the Department of Physics, Gauhati University, Guwahati - 781014, India.

1 Introduction

The latest atmospheric neutrino results based on 1117 days of data from Super Kamiokande are still consistent with a standard two neutrino oscillation $\nu_\mu \to \nu_\tau$ with a near maximal mixing angle $\sin^2 2\theta_{23} > 0.88$ and a mass square splitting Δm_{23}^2 from 1.5×10^{-3} to 5×10^{-3} eV^2 at 90% CL [1]. The sterile neutrino oscillation hypothesis $\nu_\mu \to \nu_s$ is excluded at 99% CL. Super Kamiokande is also beginning to provide important clues concerning the correct solution to the solar neutrino problem. The latest results from 1117 days of data from Super Kamiokande [2] sees a one sigma day-night asymmetry, and a flat energy spectrum, which together disfavour the small mixing angle (SMA) MSW solution [3], the just-so vacuum oscillation hypothesis [4] and the sterile neutrino hypotheses. All three possibilities are now excluded at 95% CL. The results allow much of the large mixing angle (LMA) MSW region, which now looks like the leading candidate for the solution to the solar neutrino problem. For example a typical point in the LMA MSW region is $\sin^2 2\theta_{12} \approx 0.75$ and $\Delta m_{12}^2 \approx 2.5 \times 10^{-5}$ eV^2[5].

The see-saw mechanism [6] implies that the three light neutrino masses arise from some large mass scales corresponding to the Majorana masses of some heavy "right-handed neutrinos" N_R^p M_{RR}^{pq} $(p, q = 1, \cdots, Z)$ whose entries take values which extend from $\sim 10^{14}$ GeV down to perhaps several orders of magnitude lower. The presence of electroweak scale Dirac mass terms m_{LR}^{ip} (a $3 \times Z$ matrix) connecting the left-handed neutrinos ν_L^i $(i = 1, \ldots 3)$ to the right-handed neutrinos N_R^p then results in a very light see-saw suppressed effective 3×3 Majorana mass matrix

$$m_{LL} = m_{LR} M_{RR}^{-1} m_{LR}^T \tag{1}$$

for the left-handed neutrinos ν_L^i, which are the light physical degrees of freedom observed by experiment. If the neutrino masses arise from the see-saw mechanism

then it is natural to assume the existence of a physical neutrino mass hierarchy $m_{\nu_1} \ll m_{\nu_2} \ll m_{\nu_3}$, which implies $\Delta m_{23}^2 \approx m_{\nu_3}^2$, and $\Delta m_{12}^2 \approx m_{\nu_2}^2$, which fixes $m_{\nu_3} \approx 5.6 \times 10^{-2} eV$, and (assuming the LMA MSW solution) $m_{\nu_2} \approx 5.2 \times 10^{-3} eV$, with rather large errors. Thus $m_{\nu_2}/m_{\nu_3} \sim 0.1$. In view of such a 23 mass hierarchy the presence of a large 23 mixing angle looks a bit surprising at first sight, especially given our experience with small quark mixing angles. Several explanations have been proposed [7], but the simplest idea is that the contributions to the 23 block of the light effective Majorana matrix come predominantly from a single right-handed neutrino, which causes the 23 subdeterminant to approximately vanish. This mechanism, called single right-handed neutrino dominance (SRHND), was proposed in [8], and developed for bi-maximal mixing in [9].

In this paper we shall be concerned with the effect of radiative corrections in models based on SRHND and $U(1)$ family symmetry [8], and in particular on the case of bi-maximal mixing in these models [9] . We choose these models because analytic estimates suggest that the 23 hierarchy arises from a physical mechanism which accounts for the smallness of the 23 subdeterminant, and so this hierarchy should be stable under radiative corrections. Although the radiative corrections to atmospheric mixing are only a modest 10%, this can nevertheless play an important role in achieving near maximal atmospheric mixing. Our results may be compared to the several RG studies of various models which already exist in the literature [10], [11]. Many of the existing studies do not take proper account of the heavy right-handed neutrino mass thresholds, often only including the effects of running due to the low energy dimension 5 see-saw operator from the see-saw scale down to low energies [10], or running from the high energy scale down to low energies including a single right-handed neutrino mass threshold [11], assuming that all the right-handed neutrinos are degenerate. Our results indicate that the corrections in running from the high energy scale, through the heavy neutrino threshold region, down to the

lightest right-handed neutrino mass scale are just as important (and in some cases more so) than the traditionally calculated radiative corrections in running from the lightest right-handed neutrino mass scale down to low energies.

The paper is organised as follows. In section 2 we define the MSSM with Z right-handed neutrinos, where the heavy neutrino mass matrix arises from the vacuum expectation value (VEV) of a singlet field Σ, and write down the renormalisation group equations (RGEs) relevant for running from the unification scale $M_U \sim 2 \times 10^{16} GeV$ down to low energies. In section 3 we review the analytic discussion of the phenomenological conditions for SRHND and LMA MSW involving the different types of heavy Majorana neutrino textures, and show how a $U(1)$ family symmetry may be used to satisfy them [9]. In section 4 we discuss three explicit examples of this kind, and then perform our numerical RG analysis of these cases. Section 5 concludes the paper.

2   The MSSM with Z Right-handed neutrinos

We consider the Yukawa terms with two Higgs doublets augmented by Z right-handed neutrinos, which, are given by

$$
\begin{aligned}
\mathcal{L}_{yuk} &= \epsilon_{ab}[-Y_{ij}^u H_u^a Q_i^b U_j^c + Y_{ij}^d H_d^a Q_i^b D_j^c + Y_{ij}^e H_d^a L_i^b E_j^c - Y_{ip}^\nu H_u^a L_i^b N_p^c \\
&+ \frac{1}{2} Y_{RR}^{pq} \Sigma N_p^c N_q^c] + H.c.
\end{aligned} \tag{2}
$$

where $\epsilon_{ab} = -\epsilon_{ba}$, $\epsilon_{12} = 1$, and the remaining notation is standard except that the Z right-handed neutrinos N_R^p have been replaced by their CP conjugates N_p^c with $p, q = 1, \ldots, Z$ and we have introduced a singlet field Σ whose vacuum expectation value (VEV) induces a heavy Majorana matrix $M_{RR} = < \Sigma > Y_{RR}$. When the two Higgs doublets get their VEVS $< H_u^2 >= v_2$, $< H_d^1 >= v_1$ with $\tan\beta \equiv v_2/v_1$ we find

the terms

$$\mathcal{L}_{yuk} = v_2 Y_{ij}^u U_i U_j^c + v_1 Y_{ij}^d D_i D_j^c + v_1 Y_{ij}^e E_i E_j^c + v_2 Y_{ip}^\nu N_i N_p^c + \frac{1}{2} M_{RR}^{pq} N_p^c N_q^c + H.c. \quad (3)$$

Replacing CP conjugate fields we can write in a matrix notation

$$\mathcal{L}_{yuk} = \bar{U}_L v_2 Y^u U_R + \bar{D}_L v_1 Y^d D_R + \bar{E}_L v_1 Y^e E_R + \bar{N}_L v_2 Y^\nu N_R + \frac{1}{2} N_R^T M_{RR} N_R + H.c. \quad (4)$$

where we have assumed that all the masses and Yukawa couplings are real and written $Y^* = Y$. The diagonal mass matrices are given by the following unitary transformations

$$v_2 Y_{diag}^u = V_{uL} v_2 Y^u V_{uR}^\dagger = \text{diag}(m_u, m_c, m_t),$$

$$v_1 Y_{diag}^d = V_{dL} v_1 Y^d V_{dR}^\dagger = \text{diag}(m_d, m_s, m_b),$$

$$v_1 Y_{diag}^e = V_{eL} v_1 Y^e V_{eR}^\dagger = \text{diag}(m_e, m_\mu, m_\tau),$$

$$M_{RR}^{diag} = \Omega_{RR} M_{RR} \Omega_{RR}^\dagger = \text{diag}(M_{R1}, \ldots, M_{RZ}). \quad (5)$$

Below the mass of the lightest right-handed neutrino M_{R1} the right-handed neutrino masses may be integrated out of the theory, which corresponds to replacing the last two terms in Eq.2 by a dimension 5 operator

$$- \epsilon_{ab} Y_{ip}^\nu H_u^a L_i^b N_p^c + \frac{1}{2} M_{RR}^{pq} N_p^c N_q^c + H.c. \rightarrow -\frac{1}{2} \kappa_{ij} (\epsilon_{ab} H_u^a L_i^b)(\epsilon_{a'b'} H_u^{a'} L_j^{b'}) + H.c. \quad (6)$$

where $\kappa = Y_\nu M_{RR}^{-1} Y_\nu^T$ is simply related to the see-saw mass matrix in Eq.1 when the Higgs fields are replaced by their VEVs

$$m_{LL} = v_2^2 \kappa. \quad (7)$$

Having constructed the light Majorana mass matrix it must then be diagonalised by unitary transformations,

$$m_{LL}^{diag} = V_{\nu L} m_{LL} V_{\nu L}^\dagger = \text{diag}(m_{\nu_1}, m_{\nu_2}, m_{\nu_3}). \quad (8)$$

The CKM matrix is given by

$$V_{CKM} = V_{uL}V_{dL}^{\dagger} \tag{9}$$

The leptonic analogue of the CKM matrix is the MNS matrix defined as [12]

$$V_{MNS} = V_{eL}V_{\nu L}^{\dagger}. \tag{10}$$

which may be parametrised by a sequence of three rotations about the 1,2 and 3 axes, as in the standard CKM parametrisation,

$$V_{MNS} = R_{23}R_{13}R_{12} \tag{11}$$

where

$$R_{23} = \begin{pmatrix} 1 & 0 & 0 \\ 0 & c_{23} & s_{23} \\ 0 & -s_{23} & c_{23} \end{pmatrix}, \ R_{13} = \begin{pmatrix} c_{13} & 0 & s_{13} \\ 0 & 1 & 0 \\ -s_{13} & 0 & c_{13} \end{pmatrix}, \ R_{12} = \begin{pmatrix} c_{12} & s_{12} & 0 \\ -s_{12} & c_{12} & 0 \\ 0 & 0 & 1 \end{pmatrix} \tag{12}$$

where $s_{ij} = \sin\theta_{ij}$, $c_{ij} = \cos\theta_{ij}$, and θ_{ij} refer to lepton mixing angles. Note that we completely ignore CP violating phases in this paper. From the unitarity conditions of the MNS matrix elements in Eq.11, and parametrisation in Eq.12, the mixing angles can be expressed in terms of elements of V_{MNS} as

$$S_{sol} = \sin^2 2\theta_{12} = \frac{4V_{e2}^2 V_{e1}^2}{(V_{e2}^2 + V_{e1}^2)^2}, \tag{13}$$

$$S_{at} = \sin^2 2\theta_{23} = \frac{4V_{\mu3}^2 V_{\tau3}^2}{(V_{\mu3}^2 + V_{\tau3}^2)^2} \tag{14}$$

In principle these mixing angles may not be exactly the same as those obtained from two generation analysis of the experimental results.

The renormalisation group equations (RGEs) to one-loop order are:

$$\frac{dY^u}{dt} = -\frac{1}{16\pi^2}[N_q.Y^u + Y^u.N_u + (N_{H_u})Y_u]$$

$$\frac{dY^d}{dt} = -\frac{1}{16\pi^2}[N_q.Y^d + Y^d.N_d + (N_{H_d})Y_d]$$

$$\frac{dY^\nu}{dt} = -\frac{1}{16\pi^2}[N_l.Y^\nu + Y^\nu.N_\nu + (N_{H_u})Y_\nu]$$

$$\begin{aligned}
\frac{dY^e}{dt} &= -\frac{1}{16\pi^2}[N_l.Y^e + Y^e.N_e + (N_{H_d})Y_e] \\
\frac{dY_{RR}}{dt} &= -\frac{1}{16\pi^2}[N_\nu.Y_{RR} + Y_{RR}.N_\nu + (N_\Sigma)Y_{RR}]
\end{aligned}$$

(15)

where the wavefunction anomalous dimensions are

$$\begin{aligned}
N_q &= (\frac{8}{3}g_3^2 + \frac{3}{2}g_2^2 + \frac{1}{30}g_1^2)I - Y^uY^{u\dagger} - Y^dY^{d\dagger} \\
N_u &= (\frac{8}{3}g_3^2 + \frac{8}{15}g_1^2)I - 2Y^{u\dagger}Y^u \\
N_d &= (\frac{8}{3}g_3^2 + \frac{2}{15}g_1^2)I - 2Y^{d\dagger}Y^d \\
N_l &= (\frac{3}{2}g_2^2 + \frac{3}{10}g_1^2)I - Y^eY^{e\dagger} - Y^\nu Y^{\nu\dagger} \\
N_e &= (\frac{6}{5}g_1^2)I - 2Y^{e\dagger}Y^e \\
N_\nu &= -2Y^{\nu\dagger}Y^\nu - Y_{RR}^\dagger Y_{RR} \\
N_{H_u} &= (\frac{3}{2}g_2^2 + \frac{3}{10}g_1^2) - 3Tr(Y^{u\dagger}Y^u) - Tr(Y^{\nu\dagger}Y^\nu) \\
N_{H_d} &= (\frac{3}{2}g_2^2 + \frac{3}{10}g_1^2) - 3Tr(Y^{d\dagger}Y^d) - Tr(Y^{e\dagger}Y^e) \\
N_\Sigma &= -Tr(Y_{RR}^\dagger Y_{RR})
\end{aligned}$$

(16)

where $t = \ln\mu$ (μ is the $\bar{M}S$ scale) and I is the unit matrix. The RGEs for the gauge couplings are

$$\frac{dg_i}{dt} = \frac{1}{16\pi^2}b_i g_i^3$$

(17)

where $b_i = (\frac{33}{5}, 1, -3)$.

The RGEs above are used to run the Yukawa matrices down from high energies (say the unification or string scale) down to the heaviest right-handed neutrino mass, M_{RZ}, which we assume is equal to the VEV of the Σ field. At this mass scale we perform a rotation of the right-handed neutrino fields to the basis in which M_{RR} is diagonal, according to Eq.5, so that Y^ν is replaced by $Y'^\nu = Y^\nu \Omega_{RR}^\dagger$. In this basis one then runs the remaining RGEs (apart from Y_{RR}) down through the right-handed neutrino thresholds diag($M_{RZ}, \ldots, M_{R1}$), decoupling each right-handed neutrino at

6

its mass threshold from the Y'^ν contributions which appear on the right-hand side of the RGEs. To be explicit, we replace on the right-hand sides of the RGEs,

$$Y'^\nu_{ip} \to Y'^\nu_{ip}\theta_p \qquad (18)$$

where $\theta_p = \theta(\ln\mu - \ln M_{Rp})$. For the (diagonal) Y_{RR} on the right-hand side we replace it by

$$Y_{RRpp} \to Y_{RRpp}\theta_p. \qquad (19)$$

In the next section we shall see that for the cases of interest it is not necessary to diagonalise M_{RR} in order to implement decoupling of the right-handed neutrinos, and one may remain in the basis defined by the $U(1)$ family charges, since decoupling is facilitated by the simple structures of M_{RR}.

Below the mass of the lightest right-handed neutrino one may use the RGE for κ, the coefficient of the dimension 5 neutrino mass operator,

$$\frac{d\kappa}{dt} = -\frac{1}{16\pi^2}[(6g_2^2 + \frac{6}{5}g_1^2)\kappa - 6\kappa Tr(Y^u Y^{u\dagger}) - (Y^e Y^{e\dagger})\kappa - \kappa(Y^e Y^{e\dagger})^T] \qquad (20)$$

In solving Eq.20, it is convenient to diagonalise Y^u and Y^e at the scale of the lightest right-handed neutrino, using Eqs.5, then make the approximation of keeping only the largest third family Yukawa eigenvalues. In the diagonal charged lepton basis, κ must be transformed to κ' given by

$$\kappa' = V_{eL}\kappa V_{eL}^\dagger \qquad (21)$$

then, retaining the third family t and τ Yukawa couplings only, the RGEs for the elements of κ' are given by

$$\frac{d\kappa'_{ij}}{dt} = -\frac{1}{16\pi^2}\kappa'_{ij}[6g_2^2 + \frac{6}{5}g_1^2 - 6h_t^2 - \delta_{i3}h_\tau^2 - \delta_{3j}h_\tau^2] \qquad (22)$$

Following from Eq.22 we see that the elements of $m'_{LL}(M_{R1}) = v_2^2\kappa'(M_{R1})$ at high energy are renormalised down to $m'_{LL}(m_t) = v_2^2\kappa'(m_t)$ at low energy, ignoring the

running of v_2, according to

$$m'_{LL}(m_t) = e^{\frac{6}{5}I_{g_1}}e^{6I_{g_2}}e^{-6I_t}\begin{pmatrix} m'_{LL11}(M_{R1}) & m'_{LL12}(M_{R1}) & m'_{LL13}(M_{R1})e^{-I_\tau} \\ m'_{LL21}(M_{R1}) & m'_{LL22}(M_{R1}) & m'_{LL23}(M_{R1})e^{-I_\tau} \\ m'_{LL31}(M_{R1})e^{-I_\tau} & m'_{LL32}(M_{R1})e^{-I_\tau} & m'_{LL33}(M_{R1})e^{-2I_\tau} \end{pmatrix} \tag{23}$$

where

$$I_f = \frac{1}{16\pi^2}\int_{\ln m_t}^{\ln M_{R1}} h_f^2(t)dt, \quad I_{g_i} = \frac{1}{16\pi^2}\int_{\ln m_t}^{\ln M_{R1}} g_i^2(t)dt \tag{24}$$

where $f = t, \tau$ and $i = 1, 2, 3$. In running down to m_t the charged lepton matrix will remain diagonal to good approximation, so that the low energy MNS matrix is simply given by

$$V_{MNS} = V'^\dagger_{\nu L}. \tag{25}$$

where $V'_{\nu L}$ is the matrix which diagonalises $m'_{LL}(m_t)$,

$$m'^{diag}_{LL}(m_t) = V'_{\nu L}m'_{LL}(m_t)V'^\dagger_{\nu L} = \text{diag}(\text{m}_{\nu_1}, \text{m}_{\nu_2}, \text{m}_{\nu_3}). \tag{26}$$

The mixing matrix V_{MNS} and hence neutrino mixing angles, are the running quantities which can be computed at different energy scales. For example, the running of the neutrino mixing angle relevant to the atmospheric neutrino deficit, θ_{23}, can be understood from the evolution equation

$$16\pi^2\frac{d}{dt}\sin^2 2\theta_{23} = -2\sin^2 2\theta_{23}(1 - \sin^2\theta_{23})(h_\tau^2 - h_\mu^2)\frac{m_{LL}^{33'} + m_{LL}^{22'}}{m_{LL}^{33'} - m_{LL}^{22'}} \tag{27}$$

This equation (see Babu et al in ref.[7]) describes the evolution of the physical 23 mixing angle assuming that we are in the diagonal charged lepton mass basis.

3 Three right-handed neutrinos and SRHND

We now specialise to three right-handed neutrinos and review the conditions for achieving SRHND and the LMA MSW solution [9]. The statement of SRHND is that, of the three right-handed neutrinos, one of them, N_{R3}, makes the dominant

8

contribution to the 23 block of m_{LL}. This ensures that the 23 sub-determinant approximately vanishes, and a 23 mass hierarchy therefore naturally results.

We first write the neutrino Yukawa matrix in general as

$$Y_\nu = \begin{pmatrix} a' & a & d \\ b' & b & e \\ c' & c & f \end{pmatrix} \tag{28}$$

There are now three distinct textures for the heavy Majorana neutrino matrix which maintain the isolation of the dominant right-handed neutrino N_{R3}, namely the diagonal, democratic and off-diagonal textures introduced previously[8, 9]. We consider each of them in turn. Note that, assuming SRHND, the contribution to the lepton 23 and 13 mixing angles from the neutrino sector are approximately

$$\tan\theta_{23} \approx \frac{e}{f}, \quad \tan\theta_{13} \approx \frac{d}{\sqrt{e^2 + f^2}}, \tag{29}$$

so that Super-Kamiokande and CHOOZ [13] imply

$$d \ll e \approx f \tag{30}$$

The condition on the 12 mixing angle such that it is relevant for the LMA MSW solution is discussed separately for each case below.

3.1 Diagonal Texture

$$M_{RR} = \begin{pmatrix} X' & 0 & 0 \\ 0 & X & 0 \\ 0 & 0 & Y \end{pmatrix} \tag{31}$$

We may invert the heavy Majorana matrix and construct the light Majorana matrix using the see-saw mechanism,

$$m_{LL} = \begin{pmatrix} \frac{d^2}{Y} + \frac{a^2}{X} + \frac{a'^2}{X'} & \frac{de}{Y} + \frac{ab}{X} + \frac{a'b'}{X'} & \frac{df}{Y} + \frac{ac}{X} + \frac{a'c'}{X'} \\ . & \frac{e^2}{Y} + \frac{b^2}{X} + \frac{b'^2}{X'} & \frac{ef}{Y} + \frac{bc}{X} + \frac{b'c'}{X'} \\ . & . & \frac{f^2}{Y} + \frac{c^2}{X} + \frac{c'^2}{X'} \end{pmatrix} v_2^2 \tag{32}$$

The SRHND condition is [9]

$$\frac{e^2}{Y} \sim \frac{ef}{Y} \sim \frac{f^2}{Y} \gg \frac{xy}{X}, \frac{x'y'}{X'} \tag{33}$$

9

where $x, y \in a, b, c$ and $x', y' \in a', b', c'$. [2] The 12 mixing angle determines whether we have the LMA MSW or SMA MSW solution, and this depends on the relative magnitude of the *sub-dominant* entries of m_{LL}, as discussed in [9]. The condition for LMA MSW is [9]

$$max\left(\frac{ab}{X}, \frac{ac}{X}, \frac{a'b'}{X'}, \frac{a'c'}{X'}\right) \sim max\left(\frac{b^2}{X}, \frac{bc}{X}, \frac{c^2}{X}, \frac{b'^2}{X'}, \frac{b'c'}{X'}, \frac{c'^2}{X'}\right) \qquad (34)$$

3.2   Off-Diagonal Texture

This is defined by:

$$M_{RR} = \begin{pmatrix} 0 & X & 0 \\ X & 0 & 0 \\ 0 & 0 & Y \end{pmatrix} \qquad (35)$$

The off-diagonal case is qualitatively different from the other two cases and gives

$$m_{LL} = \begin{pmatrix} \frac{d^2}{Y} + \frac{2aa'}{X} & \frac{de}{Y} + \frac{a'b}{X} + \frac{ab'}{X} & \frac{df}{Y} + \frac{a'c}{X} + \frac{ac'}{X} \\ . & \frac{e^2}{Y} + \frac{2bb'}{X} & \frac{ef}{Y} + \frac{b'c}{X} + \frac{bc'}{X} \\ . & . & \frac{f^2}{Y} + \frac{2cc'}{X} \end{pmatrix} v_2^2 \qquad (36)$$

SRHND is now defined by the conditions

$$\frac{e^2}{Y} \sim \frac{ef}{Y} \sim \frac{f^2}{Y} \gg \frac{xx'}{X} \qquad (37)$$

where $x \in a, b, c$ and $x' \in a', b', c'$, The LMA MSW solution condition is [9]:

$$max\left(\frac{a'b}{X}, \frac{ab'}{X}, \frac{a'c}{X}, \frac{ac'}{X}\right) \sim max\left(\frac{bb'}{X}, \frac{b'c}{X}, \frac{bc'}{X}, \frac{cc'}{X}\right) \qquad (38)$$

3.3   Democratic Texture

The democratic case (assuming the Majorana masses in the upper block are of the same order but are not exactly equal) is defined by:

$$M_{RR} = \begin{pmatrix} X & X & 0 \\ X & X & 0 \\ 0 & 0 & Y \end{pmatrix} \qquad (39)$$

---

[2]The beauty of SRHND is that it automatically implies $m_{\nu_2} \ll m_{\nu_3}$ due to the approximately vanishing 23 subdeterminant, without the need for appeal to cancellations. To understand this simply drop the $1/X$ terms and observe that the 23 subdeterminant vanishes which implies a massless eigenvalue which is a rather extreme case of a hierarchy!

The order of magnitude of m_{LL} is:

$$m_{LL} = \begin{pmatrix} \frac{d^2}{Y} + O(\frac{a^2}{X}) + O(\frac{a'^2}{X}) & \frac{de}{Y} + O(\frac{ab}{X}) + O(\frac{a'b'}{X}) & \frac{df}{Y} + O(\frac{ac}{X}) + O(\frac{a'c'}{X}) \\ . & \frac{e^2}{Y} + O(\frac{b^2}{X}) + O(\frac{b'^2}{X}) & \frac{ef}{Y} + O(\frac{bc}{X}) + O(\frac{b'c'}{X}) \\ . & . & \frac{f^2}{Y} + O(\frac{c^2}{X}) + O(\frac{c'^2}{X}) \end{pmatrix} v_2^2$$

(40)

In this case the SRHND conditions are:

$$\frac{e^2}{Y} \sim \frac{ef}{Y} \sim \frac{f^2}{Y} \gg \frac{xy}{X} \sim \frac{x'y'}{X}$$

(41)

where $x, y \in a, b, c$ and $x', y' \in a', b', c'$. The LMA MSW condition for a large 12 angle is

$$max\left(\frac{ab}{X}, \frac{ac}{X}, \frac{a'b'}{X}, \frac{a'c'}{X}\right) \sim max\left(\frac{b^2}{X}, \frac{bc}{X}, \frac{c^2}{X}, \frac{b'^2}{X}, \frac{b'c'}{X}, \frac{c'^2}{X}\right)$$

(42)

3.4 $U(1)$ Family Symmetry

Introducing a $U(1)$ family symmetry [14], [15], [16], [17] provides a convenient way to organise the hierarchies within the various Yukawa matrices. For definiteness we shall focus on a particular class of model based on a single pseudo-anomalous $U(1)$ gauged family symmetry [16]. We assume that the $U(1)$ is broken by the equal VEVs of two singlets $\theta, \bar{\theta}$ which have vector-like charges ± 1 [16]. The $U(1)$ breaking scale is set by $< \theta >=< \bar{\theta} >$ where the VEVs arise from a Green-Schwartz mechanism [18] with computable Fayet-Illiopoulos D-term which determines these VEVs to be one or two orders of magnitude below M_U. Additional exotic vector matter with mass M_V allows the Wolfenstein parameter [19] to be generated by the ratio [16]

$$\frac{< \theta >}{M_V} = \frac{< \bar{\theta} >}{M_V} = \lambda \approx 0.22$$

(43)

The idea is that at tree-level the $U(1)$ family symmetry only permits third family Yukawa couplings (e.g. the top quark Yukawa coupling). Smaller Yukawa couplings are generated effectively from higher dimension non-renormalisable operators corresponding to insertions of θ and $\bar{\theta}$ fields and hence to powers of the expansion parameter

11

in Eq.43, which we have identified with the Wolfenstein parameter. The number of powers of the expansion parameter is controlled by the $U(1)$ charge of the particular operator. The fields relevant to neutrino masses L_i, N_p^c, H_u, Σ are assigned $U(1)$ charges l_i, n_p, $h_u = 0$, σ. From Eqs.43, the neutrino Yukawa couplings and Majorana mass terms may then be expanded in powers of the Wolfenstein parameter,

$$M_{RR} \sim \begin{pmatrix} \lambda^{|2n_1+\sigma|} & \lambda^{|n_1+n_2+\sigma|} & \lambda^{|n_1+n_3+\sigma|} \\ . & \lambda^{|2n_2+\sigma|} & \lambda^{|n_2+n_3+\sigma|} \\ . & . & \lambda^{|2n_3+\sigma|} \end{pmatrix} <\Sigma> \qquad (44)$$

The conditions which ensure that the third dominant neutrino is isolated require that the elements $\lambda^{|n_1+n_3+\sigma|}$, $\lambda^{|n_2+n_3+\sigma|}$ be sufficiently small. The diagonal, off-diagonal and democratic textures then emerge as approximate cases [8, 9]. The neutrino Yukawa matrix is explicitly

$$Y_\nu \sim \begin{pmatrix} \lambda^{|l_1+n_1|} & \lambda^{|l_1+n_2|} & \lambda^{|l_1+n_3|} \\ \lambda^{|l_2+n_1|} & \lambda^{|l_2+n_2|} & \lambda^{|l_2+n_3|} \\ \lambda^{|l_3+n_1|} & \lambda^{|l_3+n_2|} & \lambda^{|l_3+n_3|} \end{pmatrix} \qquad (45)$$

which may be compared to the notation in Eq.28. The requirement of large 23 mixing and small 13 mixing expressed in Eq.30 becomes

$$|n_3 + l_2| = |n_3 + l_3|, \qquad |n_3 + l_1| - |n_3 + l_3| = 1 \ or \ 2 \qquad (46)$$

The remaining conditions for the $U(1)$ charges depend on the specific heavy Majorana texture under consideration [9].

The charged lepton Yukawa matrix is given by

$$Y_e \sim \begin{pmatrix} \lambda^{|l_1+e_1|} & \lambda^{|l_1+e_2|} & \lambda^{|l_1+e_3|} \\ \lambda^{|l_2+e_1|} & \lambda^{|l_2+e_2|} & \lambda^{|l_2+e_3|} \\ \lambda^{|l_3+e_1|} & \lambda^{|l_3+e_2|} & \lambda^{|l_3+e_3|} \end{pmatrix} \qquad (47)$$

where e_i are the $U(1)$ charges of the charged lepton singlet fields.

For the quarks we shall assume a common form for the textures of Y^u and Y^d

$$Y^u \sim \begin{pmatrix} \lambda^8 & \lambda^5 & \lambda^3 \\ \lambda^7 & \lambda^4 & \lambda^2 \\ \lambda^5 & \lambda^2 & 1 \end{pmatrix}, \qquad Y^d \sim \begin{pmatrix} \lambda^4 & \lambda^3 & \lambda^3 \\ \lambda^3 & \lambda^2 & \lambda^2 \\ \lambda & 1 & 1 \end{pmatrix} \lambda^n \qquad (48)$$

4   Renormalisation Group Analysis of SRHND

In [9] we tabulated the simplest charges which satisfy all the conditions given above, and so provide a natural account of the atmospheric and solar neutrinos via the LMA MSW effect. In Table 1 we consider one example of each of the three cases, namely case A (Diagonal M_{RR}), case B (Off-diagonal M_{RR}) and case C (Democratic M_{RR}). The $U(1)$ charges along with corresponding M_{RR}, Y^ν, obtained from Eqs.44, 45, and other relevant parameters are outlined for each case, including the charged lepton charges, are also shown. Note that the zeroes in M_{RR} appear after small angle rotations on the right-handed neutrino fields, which will not affect the perturbative expansion in powers of λ in Y^ν. The order unity coefficients b_{ij}, which are always present in $U(1)$ models, are defined in this basis.

In case A, before rotating to the diagonal charged lepton mass basis, we may easily estimate the order of the entries in m_{LL} in Eq.32 from the matrices Y^ν and M_{RR} in Table 1, and hence verify the SRHND conditions Eq.33, and the LMA MSW condition Eq.34. Using Eq.32 we find

$$m_{LL} \sim \begin{pmatrix} \lambda + \lambda + \lambda & 1 + \lambda + \lambda^2 & 1 + \lambda + \lambda^2 \\ . & \frac{1}{\lambda} + \lambda + \lambda^3 & \frac{1}{\lambda} + \lambda + \lambda^3 \\ . & . & \frac{1}{\lambda} + \lambda + \lambda^3 \end{pmatrix} \frac{v_2^2}{<\Sigma>} \tag{49}$$

where the first entry in each element corresponds to the $1/Y$ contributions from N_{3R}, which clearly dominate the 23 block by a factor of λ^2, and the 12 and 13 elements by a factor of λ. The 13 element is smaller than the elements in the 23 block by a factor of λ leading to a 13 CHOOZ angle of this order. The subdominant entries in the 12,13,22,23 elements are the same order, leading to a large 12 angle suitable for LMA MSW.

Similarly in case B, we can show that the SRHND condition Eq.37 and LMA MSW condition Eq.38 are satisfied. We estimate the order of the entries in m_{LL} in

Parameter	Case A (Diagonal M_{RR})	Case B (Off-diagonal M_{RR})	Case C (Democratic M_{RR})
$U(1)$ charges	$l_{1,2,3} = -1, 1, 1$ $n_{1,2,3} = 1/2, 0, -1/2$ $e_{1,2,3} = -3, -3, -1,$ $\sigma = -1$	$l_{1,2,3} = -2, 0, 0$ $n_{1,2,3} = -2, 1, -1$ $e_{1,2,3} = -2, -2, 0,$ $\sigma = 1$	$l_{1,2,3} = -1, 1, 1,$ $n_{1,2,3} = 0, 0, -1/2$ $e_{1,2,3} = -3, -3, -1,$ $\sigma = -1$
Y^e	$\begin{pmatrix} a_{11}\lambda^4 & a_{12}\lambda^4 & a_{13}\lambda^2 \\ a_{21}\lambda^2 & a_{22}\lambda^2 & a_{23} \\ a_{31}\lambda^2 & a_{32}\lambda^2 & a_{33} \end{pmatrix}$	$\begin{pmatrix} a_{11}\lambda^4 & a_{12}\lambda^4 & a_{13}\lambda^2 \\ a_{21}\lambda^2 & a_{22}\lambda^2 & a_{23} \\ a_{31}\lambda^2 & a_{32}\lambda^2 & a_{33} \end{pmatrix}$	$\begin{pmatrix} a_{11}\lambda^4 & a_{12}\lambda^4 & a_{13}\lambda^2 \\ a_{21}\lambda^2 & a_{22}\lambda^2 & a_{23} \\ a_{31}\lambda^2 & a_{32}\lambda^2 & a_{33} \end{pmatrix}$
a_{ij}	$\begin{pmatrix} 0.9 & 1.25 & 0.85 \\ 1.2 & 4.2 & 1.25 \\ 0.85 & 1.6 & 1.0 \end{pmatrix}$	$\begin{pmatrix} 0.9 & 1.25 & 0.85 \\ 1.2 & 4.2 & 1.25 \\ 0.85 & 1.6 & 1.0 \end{pmatrix}$	$\begin{pmatrix} 0.9 & 1.25 & 0.85 \\ 1.2 & 4.2 & 1.25 \\ 0.85 & 1.6 & 1.0 \end{pmatrix}$
Y^ν	$\begin{pmatrix} b_{11}\lambda^{\frac{1}{2}} & b_{12}\lambda & b_{13}\lambda^{\frac{3}{2}} \\ b_{21}\lambda^{\frac{3}{2}} & b_{22}\lambda & b_{23}\lambda^{\frac{1}{2}} \\ b_{31}\lambda^{\frac{3}{2}} & b_{32}\lambda & b_{33}\lambda^{\frac{1}{2}} \end{pmatrix}$	$\begin{pmatrix} b_{11}\lambda^4 & b_{12}\lambda & b_{13}\lambda^3 \\ b_{21}\lambda^2 & b_{22}\lambda & b_{23}\lambda \\ b_{31}\lambda^2 & b_{32}\lambda & b_{33}\lambda \end{pmatrix}$	$\begin{pmatrix} b_{11}\lambda & b_{12}\lambda & b_{13}\lambda^{\frac{3}{2}} \\ b_{21}\lambda & b_{22}\lambda & b_{23}\lambda^{\frac{1}{2}} \\ b_{31}\lambda & b_{32}\lambda & b_{33}\lambda^{\frac{1}{2}} \end{pmatrix}$
b_{ij}	$\begin{pmatrix} 0.5 & 0.85 & 1.0 \\ 1.0 & 1.3 & 0.4 \\ 1.1 & 0.4 & 1.5 \end{pmatrix}$	$\begin{pmatrix} 1.0 & 1.8 & 1.35 \\ 1.8 & 1.35 & 0.4 \\ 1.0 & 0.4 & 1.6 \end{pmatrix}$	$\begin{pmatrix} 0.5 & 0.85 & 1.0 \\ 1.0 & 1.3 & 0.5 \\ 1.1 & 0.5 & 1.5 \end{pmatrix}$
$\frac{M_{RR}}{<\Sigma>}$	$\begin{pmatrix} 1 & 0 & 0 \\ 0 & \lambda & 0 \\ 0 & 0 & \lambda^2 \end{pmatrix}$	$\begin{pmatrix} 0 & 1 & 0 \\ 1 & 0 & 0 \\ 0 & 0 & \lambda \end{pmatrix}$	$\begin{pmatrix} \lambda & c_{12}\lambda & 0 \\ c_{12}\lambda & \lambda & 0 \\ 0 & 0 & \lambda^2 \end{pmatrix}$
$<\Sigma>$	$22.75 \times 10^{14} GeV$	$2.20 \times 10^{14} GeV$	$38.20 \times 10^{14} GeV$
M_{R_1}	$1.10 \times 10^{14} GeV$	$4.84 \times 10^{13} GeV$	$1.85 \times 10^{14} GeV$
$I_{g_{1,2}}$ $I_{t,\tau}$ $I_{\mu,e}$	$0.048918, 0.0751076$ $0.133729, 0.118012$ $4.1884.10^{-4}, 1.794.10^{-8}$	$0.046789, 0.072753$ $0.130667, 0.111514$ $4.0474.10^{-4}, 1.711.10^{-8}$	$0.0498926, 0.07625$ $0.135464, 0.120819$ $4.278.10^{-4}, 1.829.10^{-8}$

Table 1: Textures of the Yukawa couplings of Dirac neutrino mass, right-handed Majorana neutrino mass, and also other relevant parameters (as defined in the text) required for the numerical estimation of left-handed Majorana neutrino masses at low energies through see-saw mechanism in tables 2,3 and 4. $<\Sigma>$ is taken as a free parameter and M_{R_1} is the lowest threshold scale in M_{RR}. We take $c_{12} \approx 0.9$.

Eq.36 from the matrices Y^ν and M_{RR} in Table 1 as,

$$m_{LL} \sim \begin{pmatrix} \lambda^5 + 2\lambda^5 & \lambda^3 + \lambda^5 + \lambda^3 & \lambda^3 + \lambda^5 + \lambda^3 \\ . & \lambda + 2\lambda^3 & \lambda + \lambda^3 + \lambda^3 \\ . & . & \lambda + 2\lambda^3 \end{pmatrix} \frac{v_2^2}{<\Sigma>} \qquad (50)$$

where the first entry in each element corresponds to the $1/Y$ contributions coming from the right-handed neutrino N_{3R}, and clearly dominates the 23 block by a factor of λ^2. In this case it does not dominate the other elements outside the 23 block. The 13 element from N_{3R} is suppressed relative to the 23 block elements by a factor of λ^2, leading to a CHOOZ angle of this order. The subdominant entries in the 12,13,22,23 elements are again the same order, leading to a large 12 angle suitable for LMA MSW.

Finally in case C, we verify that the SRHND condition Eq.41 and LMA MSW condition Eq.42 are satisfied, by constructing the entries in m_{LL} in Eq.40 from the matrices Y^ν and M_{RR} in Table 1,

$$m_{LL} \sim \begin{pmatrix} \lambda + \lambda + \lambda & 1 + \lambda + \lambda & 1 + \lambda + \lambda \\ . & \frac{1}{\lambda} + \lambda + \lambda & \frac{1}{\lambda} + \lambda + \lambda \\ . & . & \frac{1}{\lambda} + \lambda + \lambda \end{pmatrix} \frac{v_2^2}{<\Sigma>} \qquad (51)$$

where the first entry in each element corresponds to the $1/Y$ contributions coming from the dominant right-handed neutrino, which dominates in the 23 block by a factor of λ^2 and in the 12 and 13 elements by a factor of λ. The 13 element is smaller than the 23 elements by a factor of λ leading to a CHOOZ angle of this order. The subdominant 12,13,22,23 elements are all the same order leading to LMA MSW.

We now turn to a numerical treatment of these three cases. In integrating the RGEs down to low energies the heavy thresholds for the diagonal texture in Eq.31 are dealt with exactly as described in the previous section, except that no rotation is required to get to the diagonal M_{RR} basis since we already begin with that form. For the democratic texture in Eq.39 there are essentially only two mass thresholds to consider X and Y since N_{R1} and N_{R2} are approximately degenerate with mass X and we can ignore any small mass difference between them to leading order. Similarly for

the off-diagonal texture in Eq.35 we also have only two mass thresholds to consider X and Y since N_{R1} and N_{R2} are now exactly degenerate with mass X. Thus for both democratic and off-diagonal textures we can replace on the right-hand sides of the RGEs by

$$Y_{i1}^\nu \to Y_{i1}^\nu \theta_1, \quad Y_{i2}^\nu \to Y_{i2}^\nu \theta_2, \quad Y_{i3}^\nu \to Y_{i3}^\nu \theta_3 \tag{52}$$

where $\theta_{1,2} = \theta(\ln \mu - \ln X)$, $\theta_3 = \theta(\ln \mu - \ln Y)$. We replace Y_{RR} on the right-hand side of the RGEs by

$$Y_{RRij} \to Y_{RRij}\theta_i\theta_j. \tag{53}$$

Tables 2-4 give the numerical values of quantities at three different energy scales: the GUT scale $M_U = 2.0 \times 10^{16}$ GeV, the lightest right-handed neutrino mass $M_{R_1} \sim 10^{14}$ GeV, and the low energy scale $m_t = 175$ GeV. To begin with the left-handed Majorana neutrino mass matrix [3] $m_{LL}(M_X)$ arising from the sum of dominant and subdominant contributions from N_{R3} and N_{R1}, N_{R2} respectively, are numerically computed at the energy scale $\mu = M_U = 2.0 \times 10^{16}$GeV, as seen in tables 2,3,4 for the three cases (A,B,C) for large $\tan\beta$. The corresponding MNS mixing matrices which in turn give S_{sol} and S_{at} along with neutrino masses $(m_{\nu 1}, m_{\nu 2}, m_{\nu 3})$ are also estimated. Next, as already discussed in section 2, we calculate the radiative corrections to m'_{LL} and V_{MNS} through the running of the Yukawa couplings Y^u, Y^d, Y^ν, Y^e, Y_{RR}, and the gauge couplings g_1, g_2, g_3 from high energy scale M_U through the heavy neutrino threshold region at successive steps down to the lightest right-handed neutrino mass (M_{R_1}). The corresponding $m'_{LL}(M_{R_1})$ (in the diagonal charged lepton basis) and $V_{MNS}(M_{R_1})$ are again estimated as shown in tables 2,3 and 4 for three cases. Further, the radiative corrections to m'_{LL} and V_{MNS} from the lightest right-handed neutrino down to low energies (say top-quark mass scale m_t) are taken in the usual way through the running of the coefficient of the dimension 5 operator κ'

---

[3]Strictly speaking the see-saw mechanism does not operate at energy scales higher than the right-handed neutrino mass scales, but such results do provide a meaningful measure of the effects of radiative corrections from the GUT scale down to low energies.

Scale $\mu = M_U = 2.0 \times 10^{16} GeV$	Scale $\mu = M_U = 2.0 \times 10^{16} GeV$
$Y^e =$ $\begin{pmatrix} 2.114.10^{-3} & 2.928.10^{-3} & 4.114.10^{-2} \\ 5.808.10^{-2} & 0.20328 & 1.250 \\ 4.114.10^{-2} & 7.744.10^{-2} & 1.000 \end{pmatrix}$ $Y^e_{diag} = diag(4.36.10^{-4}, 6.61.10^{-2}, 1.62)$ $m'^{\nu}_{LL} =$ $\begin{pmatrix} 4.192.10^{-3} & 7.724.10^{-3} & 1.534.10^{-2} \\ 7.724.10^{-3} & 5.345.10^{-2} & 6.894.10^{-2} \\ 1.534.10^{-2} & 6.894.10^{-2} & 9.965.10^{-2} \end{pmatrix}$ $m'^{diag}_{LL} = diag(2.46 \times 10^{-4}, 0.00582, 0.151)$	$V_{eL} =$ $\begin{pmatrix} 0.999 & 0.002 & -0.044 \\ 0.036 & -0.621 & 0.783 \\ 0.026 & 0.784 & 0.620 \end{pmatrix}$ $m_e/m_\mu, m_\mu/m_\tau = 0.0066, 0.041$ $V_{MNS} = V_{eL}V^{\dagger}_{\nu L} =$ $\begin{pmatrix} 0.797 & -0.593 & 0.115 \\ 0.432 & 0.692 & 0.579 \\ -0.422 & -0.412 & 0.808 \end{pmatrix}$ $S_{sol} = 0.9173, S_{at} = 0.8965$
Scale $\mu = M_{R_1} = 1.10 \times 10^{14} GeV$	Scale $\mu = M_{R_1} = 1.10 \times 10^{14} GeV$
$Y^e =$ $\begin{pmatrix} 1.411.10^{-3} & 1.358.10^{-3} & 2.621.10^{-2} \\ 4.234.10^{-2} & 0.15298 & 0.90295 \\ 2.890.10^{-2} & 4.766.10^{-2} & 0.71419 \end{pmatrix}$ $Y^e_{diag} = diag(3.74.10^{-4}, 5.72.10^{-2}, 1.16)$ $m'^{\nu}_{LL} =$ $\begin{pmatrix} 3.827.10^{-3} & 6.800.10^{-3} & 1.278.10^{-2} \\ 6.800.10^{-3} & 4.848.10^{-2} & 5.755.10^{-2} \\ 1.278.10^{-2} & 5.755.10^{-2} & 7.715.10^{-2} \end{pmatrix}$ $m'^{diag}_{LL} = diag(2.294.10^{-4}, 0.0054, 0.1238)$	$V_{eL} =$ $\begin{pmatrix} 0.996 & 0.004 & -0.042 \\ 0.035 & -0.615 & 0.787 \\ 0.023 & 0.788 & 0.615 \end{pmatrix}$ $m_e/m_\mu, m_\mu/m_\tau = 0.0065, 0.049$ $V_{MNS} = V_{eL}V^{\dagger}_{\nu L} =$ $\begin{pmatrix} 0.790 & -0.602 & 0.118 \\ 0.421 & 0.671 & 0.606 \\ -0.446 & -0.432 & 0.784 \end{pmatrix}$ $S_{sol} = 0.92991, S_{at} = 0.9366$
Scale $\mu = m_t = 175 GeV$	Scale $\mu = m_t = 175 GeV$
$Y^e_{diag} = diag(2.89.10^{-4}, 4.41.10^{-2}, 0.627)$ $m'^{\nu}_{LL} =$ $\begin{pmatrix} 2.855.10^{-3} & 5.073.10^{-3} & 8.474.10^{-3} \\ 5.073.10^{-3} & 3.616.10^{-2} & 3.816.10^{-2} \\ 8.474.10^{-3} & 3.816.10^{-2} & 4.545.10^{-2} \end{pmatrix}$ $m'^{diag}_{LL} = diag(1.62 \times 10^{-4}, 0.003848, 0.08046)$	$m_e/m_\mu, m_\mu/m_\tau = 0.0065, 0.0703$ $V_{MNS} = V^{\dagger}_{\nu L} =$ $\begin{pmatrix} 0.768 & -0.628 & 0.124 \\ 0.412 & 0.633 & 0.656 \\ -0.490 & -0.453 & 0.745 \end{pmatrix}$ $S_{sol} = 0.9606, S_{at} = 0.9840$

Table 2: Results for case A. Left-handed Majorana neutrino mass matrix in the diagonal charged lepton basis and the MNS mixing matrix at different energy scales M_U, M_{R_1}, m_t for the case of diagonal M_{RR}. Neutrino masses are expressed in eV.

Scale $\mu = M_U = 2.0 \times 10^{16} GeV$	Scale $\mu = M_U = 2.0 \times 10^{16} GeV$
$Y^e =$ $\begin{pmatrix} 2.114.10^{-3} & 2.928.10^{-3} & 4.114.10^{-2} \\ 5.808.10^{-2} & 0.20328 & 1.250 \\ 4.114.10^{-2} & 7.744.10^{-2} & 1.000 \end{pmatrix}$ $Y^e_{diag} = diag(4.36.10^{-4}, 6.61.10^{-2}, 1.62)$ $m''^{\nu}_{LL} =$ $\begin{pmatrix} 4.457.10^{-5} & -9.965.10^{-4} & 5.172.10^{-3} \\ -9.965.10^{-4} & 3.116.10^{-2} & 3.784.10^{-2} \\ 5.172.10^{-3} & 3.784.10^{-2} & 5.983.10^{-2} \end{pmatrix}$ $m'^{diag}_{LL} = diag(-0.21 \times 10^{-2}, 0.00701, 0.086)$	$V_{eL} =$ $\begin{pmatrix} 0.999 & 0.002 & -0.044 \\ 0.036 & -0.621 & 0.783 \\ 0.026 & 0.784 & 0.620 \end{pmatrix}$ $m_e/m_\mu, m_\mu/m_\tau = 0.0066, 0.041$ $V_{MNS} = V_{eL} V^{\dagger}_{\nu L} =$ $\begin{pmatrix} 0.886 & -0.462 & 0.042 \\ 0.363 & 0.740 & 0.566 \\ -0.296 & -0.485 & 0.823 \end{pmatrix}$ $S_{sol} = 0.6731, S_{at} = 0.8918$
Scale $\mu = M_{R_1} = 4.84 \times 10^{13} GeV$	Scale $\mu = M_{R_1} = 4.84 \times 10^{13} GeV$
$Y^e =$ $\begin{pmatrix} 1.358.10^{-3} & 1.166.10^{-3} & 2.527.10^{-2} \\ 4.072.10^{-2} & 0.148 & 0.868 \\ 2.803.10^{-2} & 4.548.10^{-2} & 0.6940 \end{pmatrix}$ $Y^e_{diag} = diag(3.67.10^{-4}, 5.64.10^{-2}, 1.12)$ $m''^{\nu}_{LL} =$ $\begin{pmatrix} -1.733.10^{-5} & -1.113.10^{-3} & 4.481.10^{-3} \\ -1.113.10^{-3} & 2.972.10^{-2} & 3.333.10^{-2} \\ 4.481.10^{-3} & 3.333.10^{-2} & 4.907.10^{-2} \end{pmatrix}$ $m'^{diag}_{LL} = diag(-2.035.10^{-3}, 0.00659, 0.0742)$	$V_{eL} =$ $\begin{pmatrix} 0.999 & 0.005 & -0.043 \\ 0.037 & -0.620 & 0.784 \\ 0.023 & 0.785 & 0.619 \end{pmatrix}$ $m_e/m_\mu, m_\mu/m_\tau = 0.0065, 0.0503$ $V_{MNS} = V_{eL} V^{\dagger}_{\nu L} =$ $\begin{pmatrix} 0.882 & -0.469 & 0.039 \\ 0.355 & 0.718 & 0.598 \\ -0.309 & -0.514 & 0.800 \end{pmatrix}$ $S_{sol} = 0.6875, S_{at} = 0.9201$
Scale $\mu = m_t = 175 GeV$	Scale $\mu = m_t = 175 GeV$
$Y^e_{diag} = diag(2.85.10^{-4}, 4.39.10^{-2}, 0.619)$ $m''^{\nu}_{LL} =$ $\begin{pmatrix} -1.295.10^{-5} & -8.317.10^{-4} & 2.995.10^{-3} \\ -8.317.10^{-4} & 2.221.10^{-2} & 2.228.10^{-2} \\ 2.995.10^{-3} & 2.228.10^{-2} & 2.934.10^{-2} \end{pmatrix}$ $m'^{diag}_{LL} = diag(-1.486 \times 10^{-3}, 0.00462, 0.0484)$	$m_e/m_\mu, m_\mu/m_\tau = 0.0065, 0.0709$ $V_{MNS} = V^{\dagger}_{\nu L} =$ $\begin{pmatrix} 0.876 & 0.480 & 0.036 \\ 0.346 & -0.680 & 0.647 \\ -0.335 & 0.555 & 0.762 \end{pmatrix}$ $S_{sol} = 0.7102, S_{at} = 0.9738$

Table 3: Results for case B. Left-handed Majorana neutrino mass matrix in the diagonal charged lepton basis and the MNS mixing matrix at different energy scales M_U, M_{R_1}, m_t for the case of off-diagonal M_{RR}. Neutrino masses are expressed in eV.

Scale $\mu = M_U = 2.0 \times 10^{16} GeV$	Scale $\mu = M_U = 2.0 \times 10^{16} GeV$
$Y^e =$ $\begin{pmatrix} 2.114.10^{-3} & 2.928.10^{-3} & 4.114.10^{-2} \\ 5.808.10^{-2} & 0.20328 & 1.250 \\ 4.114.10^{-2} & 7.744.10^{-2} & 1.000 \end{pmatrix}$ $Y^e_{diag} = diag(4.36.10^{-4}, 6.61.10^{-2}, 1.62)$ $m''^{\nu}_{LL} =$ $\begin{pmatrix} 2.751.10^{-3} & 2.878.10^{-3} & 8.715.10^{-3} \\ 2.878.10^{-3} & 3.070.10^{-2} & 4.222.10^{-2} \\ 8.715.10^{-3} & 4.222.10^{-2} & 6.736.10^{-2} \end{pmatrix}$ $m'^{diag}_{LL} = diag(2.96 \times 10^{-5}, 0.00488, 0.096)$	$V_{eL} =$ $\begin{pmatrix} 0.999 & 0.002 & -0.044 \\ 0.036 & -0.621 & 0.783 \\ 0.026 & 0.784 & 0.620 \end{pmatrix}$ $m_e/m_\mu, m_\mu/m_\tau = 0.0066, 0.041$ $V_{MNS} = V_{eL}V^{\dagger}_{\nu L} =$ $\begin{pmatrix} 0.780 & -0.619 & 0.095 \\ 0.480 & 0.688 & 0.544 \\ -0.402 & -0.379 & 0.834 \end{pmatrix}$ $S_{sol} = 0.9488, S_{at} = 0.8378$
Scale $\mu = M_{R_1} = 1.85 \times 10^{14} GeV$	Scale $\mu = M_{R_1} = 1.85 \times 10^{14} GeV$
$Y^e =$ $\begin{pmatrix} 1.391.10^{-3} & 1.274.10^{-3} & 2.572.10^{-2} \\ 4.293.10^{-2} & 0.1550 & 0.9159 \\ 2.935.10^{-2} & 4.864.10^{-2} & 0.7248 \end{pmatrix}$ $Y^e_{diag} = diag(3.77.10^{-4}, 5.77.10^{-2}, 1.18)$ $m''^{\nu}_{LL} =$ $\begin{pmatrix} 2.433.10^{-3} & 2.426.10^{-3} & 7.009.10^{-3} \\ 2.426.10^{-3} & 2.753.10^{-2} & 3.471.10^{-2} \\ 7.009.10^{-3} & 3.471.10^{-2} & 5.094.10^{-2} \end{pmatrix}$ $m'^{diag}_{LL} = diag(2.674.10^{-5}, 0.00433, 0.07647)$	$V_{eL} =$ $\begin{pmatrix} 0.999 & 0.005 & -0.041 \\ 0.035 & -0.616 & 0.787 \\ 0.022 & 0.788 & 0.615 \end{pmatrix}$ $m_e/m_\mu, m_\mu/m_\tau = 0.0065, 0.049$ $V_{MNS} = V_{eL}V^{\dagger}_{\nu L} =$ $\begin{pmatrix} 0.771 & -0.630 & 0.096 \\ 0.472 & 0.665 & 0.578 \\ -0.428 & -0.401 & 0.810 \end{pmatrix}$ $S_{sol} = 0.9604, S_{at} = 0.8945$
Scale $\mu = m_t = 175 GeV$	Scale $\mu = m_t = 175 GeV$
$Y^e_{diag} = diag(2.89.10^{-4}, 4.41.10^{-2}, 0.626)$ $m''^{\nu}_{LL} =$ $\begin{pmatrix} 1.811.10^{-3} & 1.805.10^{-3} & 4.623.10^{-3} \\ 1.805.10^{-3} & 2.049.10^{-2} & 2.289.10^{-2} \\ 4.623.10^{-3} & 2.289.10^{-2} & 2.978.10^{-2} \end{pmatrix}$ $m'^{diag}_{LL} = diag(1.90 \times 10^{-5}, 0.00309, 0.04897)$	$m_e/m_\mu, m_\mu/m_\tau = 0.0065, 0.0703$ $V_{MNS} = V^{\dagger}_{\nu L} =$ $\begin{pmatrix} 0.752 & -0.652 & 0.099 \\ 0.461 & 0.628 & 0.627 \\ -0.471 & -0.426 & 0.772 \end{pmatrix}$ $S_{sol} = 0.9798, S_{at} = 0.9579$

Table 4: Results for case C. Left-handed Majorana neutrino mass matrix in the diagonal charged lepton basis and the MNS mixing matrix at different energy scales M_U, M_{R_1}, m_t for the case of democratic M_{RR}. Neutrino masses are expressed in eV.

in the diagonal charged lepton basis. These low energy results in tables 2,3,4 can be compared with observational data, and S_{sol}, S_{at} defined in Eqs.13,14 and the neutrino masses given as the diagonal elements of $m_{LL}'^{diag}$ are seen to be in good agreement with atmospheric data and the LMA MSW solutions. The CHOOZ constraint is also satisfied in all cases, with the 13 element of V_{MNS} being larger for cases A and C than for case B, as expected from the analaytical estimates above. The charged lepton mass ratios are $m_e/m_\mu \approx 0.0066$ and $m_\mu/m_\tau \approx 0.07$ at low energy scale, compared to the experimental values 0.005 and 0.06, respectively.

It is instructive to examine the RG evolution of the neutrino masses and mixing angles. The numerical results in Tables 1-4 show that neutrino masses m_{ν_2} and m_{ν_3} are decreasing from high energy scale M_U to low energy scale m_t by about 40%, but the ratios m_{ν_2}/m_{ν_3} increase by about (24%, 17%, 55%) corresponding to low energy ratios of (0.05, 0.10, 0.08) for cases (A,B,C), respectively. The atmospheric mixing quantity S_{at} increases by about 10% in the three cases, and approaches maximal mixing in all cases. This can be understood from Eq.27, which shows that in the diagonal charged lepton basis, the sign of the RGE evolution is determined by the sign of $m_{LL}^{33'} - m_{LL}^{22'}$, which in the examples in Tables 2,3,4 is always positive. This means that the overall sign of the RGE is negative, which implies an increasing S_{at} as the energy scale is reduced. Note that the largest contribution to the atmospheric mixing angle arises from the charged lepton sector, for this choice of parameters, as is clear from examining V_{eL} in Tables 2,3,4. The solar mixing quantity S_{sol} also increases, but the increases of $1 - 5\%$ are mild in comparison to S_{at}. In cases A,C S_{sol} approaches maximal mixing, while in case B its low energy value is about 0.71, which are well near the best fit $sin^2 2\theta_{12} \approx 0.76$.

In Figures 1-3 we display the RG running of the mixing angles S_{sol} and S_{at} and the ratio of neutrino masses $m_{\nu 2}/m_{\nu 3}$ as a function of $t = \ln \mu$, for the three cases

20

A,B,C. We prefer to show the variation in the neutrino mass ratio, rather than the absolute values of the two neutrino mass eigenvalues since they will depend to some extent on the running vacuum expectation value, although the effect on the present analysis is not large since we assume high $\tan\beta$. We also do not consider the ratio $m_{\nu1}/m_{\nu2}$ since this is not experimentally measurable in the hierarchical case.

In Figure 1(a) we show the variations of S_{sol} and S_{at} with energy scale for case A. As already stated, the atmospheric mixing angle runs more rapidly than the solar mixing angle, and although S_{at} starts out smaller then S_{sol} at M_U, it quickly grows larger. Note the effect of the heavy right-handed neutrino mass thresholds which change the slope of the curves, which grow steeply over the heavy threshold region. In Figure 1(b) we give the variation of the neutrino mass ratio $m_{\nu2}/m_{\nu3}$ with $t = \ln\mu$ for case A. Here the effects of the three heavy right-handed neutrino thresholds is clearly seen, with again a steep rise in this mass ratio over the heavy threshold region.

In Figure 2(a) we show the variations of S_{sol} and S_{at} with energy scale for case B. Here the atmospheric angle starts out larger than the solar angle, but still grows more rapidly. In Figure 2(b) we give the variation of the neutrino mass ratio $m_{\nu2}/m_{\nu3}$ with $t = \ln\mu$ for case B. The qualitative shape of this curve is similar to Figure 1(b), but there are only two heavy neutrino mass thresholds in this case, and also the mass ratio is larger throughout.

In Figure 3(a) we show the variations of S_{sol} and S_{at} with energy scale for case B. Here the solar angle starts out much larger than the atmospheric angle, and as before the atmospheric angle grows more rapidly and approaches the solar angle. In Figure 3(b) we give the variation of the neutrino mass ratio $m_{\nu2}/m_{\nu3}$ with $t = \ln\mu$ for case B. Because of the choice of c_{12} in Table 1, the two heavy right-handed neutrino mass thresholds are very close together in this case.
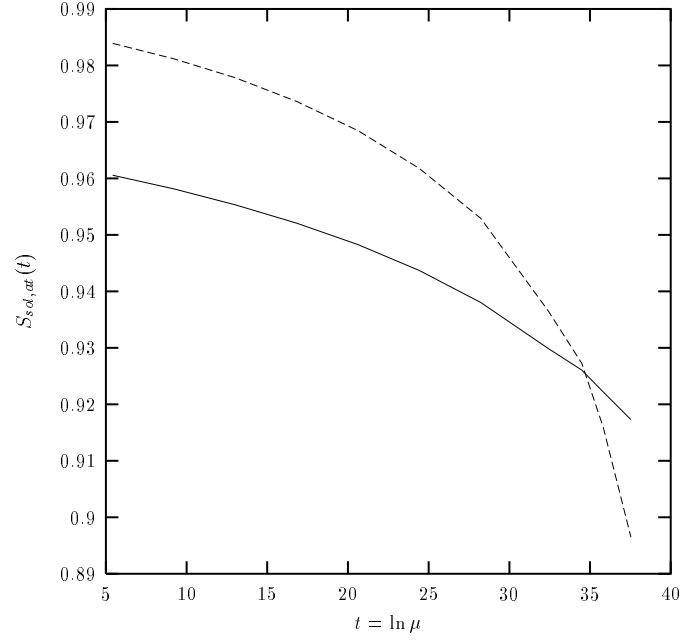
Fig.1(a) Case A (Diagonal M_{RR}): Variation of S_{sol} and S_{at} with energy scale $t = \ln \mu$, which are represented by solid-line and dotted-line respectively.
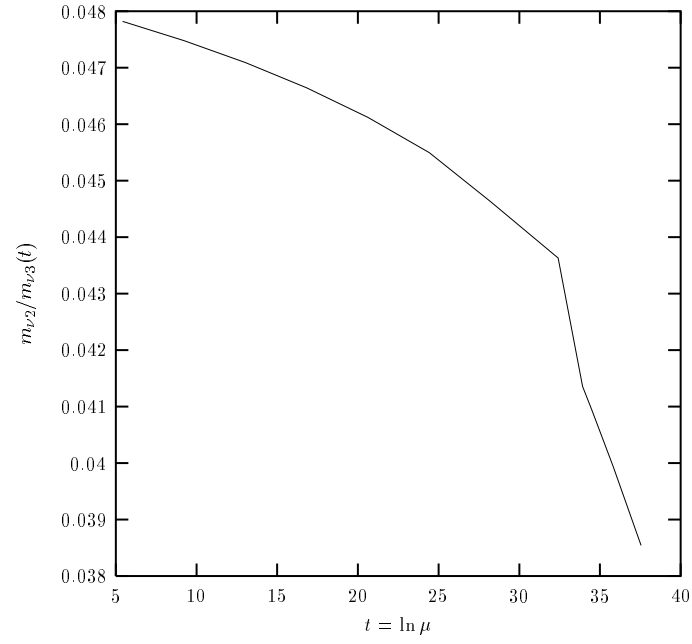

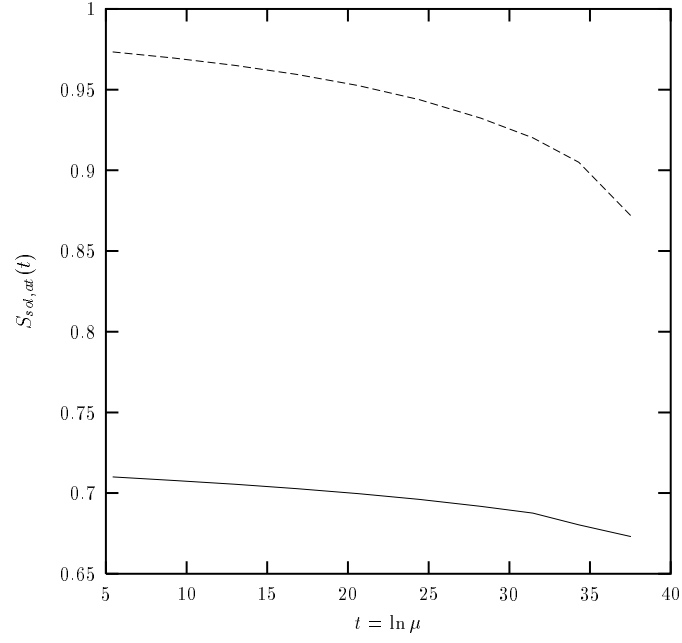Fig.1(b) Case A (Diagonal M_{RR}): Variation of the neutrino mass ratio $m_{\nu 2}/m_{\nu 3}$ with $t = \ln \mu$.

Fig.2(a) Case B (Off-diagonal M_{RR}): Variation of S_{sol} and S_{at} with $t = \ln \mu$, which are represented by solid-line and dotted-line respectively.
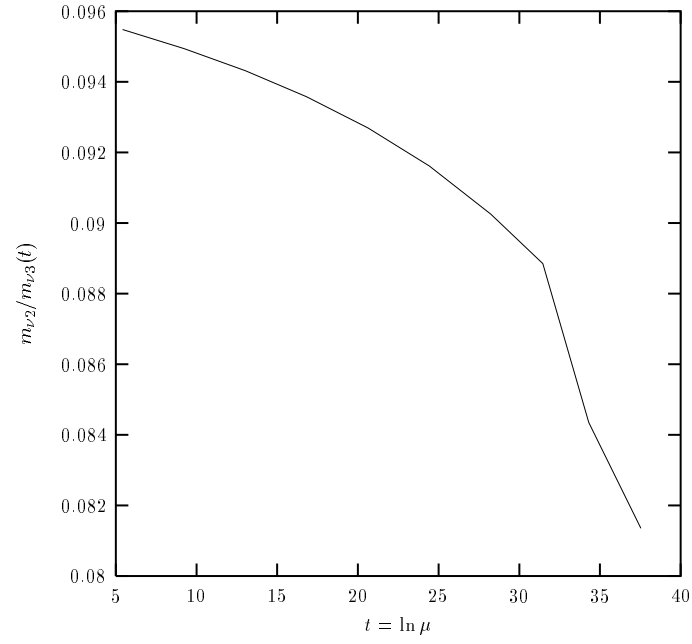

Fig.2(b) Case B (Off-diagonal M_{RR}): Variation of the neutrino mass ratio $m_{\nu 2}/m_{\nu 3}$ with $t = \ln \mu$.
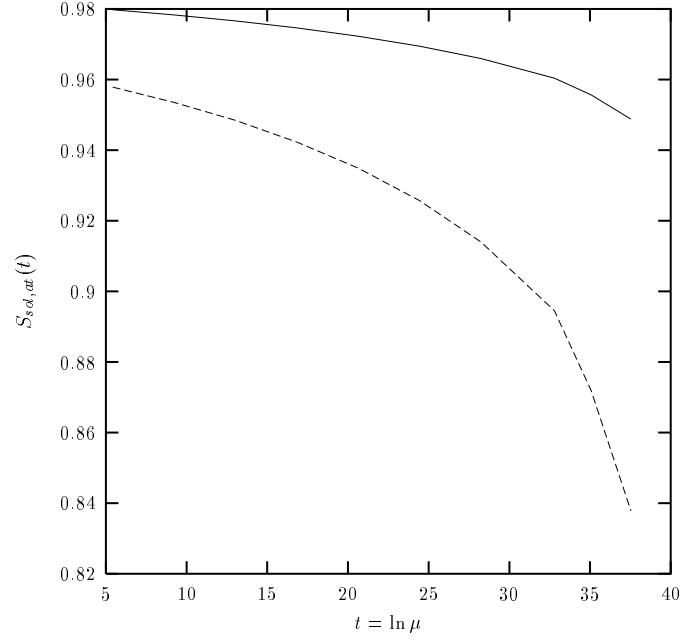
Fig.3(a) Case C (Democratic M_{RR}): Variation of S_{sol} and S_{at} with energy scale $t = \ln \mu$, which are represented by solid-line and dotted-line respectively.
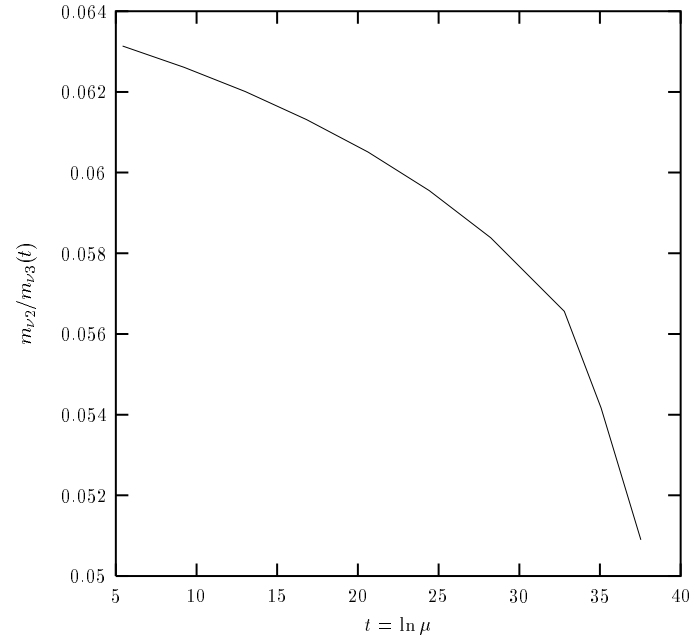

Fig.3(b) Case C (Democratic M_{RR}): Variation of the neutrino mass ratio $m_{\nu 2}/m_{\nu 3}$ with $t = \ln \mu$.

It is important to emphasise that more than 50% of the radiative corrections to all the physical quantities m_{ν_2}/m_{ν_3}, S_{at}, S_{sol} arises from the RG evolution over the range from the GUT scale $M_U = 2.0 \times 10^{16}$GeV through the heavy right-handed neutrino threshold region down to the lightest right-handed neutrino mass scale $M_{R_1} \sim 10^{14}$GeV. Therefore even though this range covers only two orders of magnitude in energy, it is just as important as the RG evolution effects from $M_{R_1} \sim 10^{14}$GeV down to low energies which covers over 12 orders of magnitude in energy, and is the region commonly considered in the literature.

5   Conclusion

We have studied the effects of radiative corrections on neutrino masses and mixing angles, in evolving the theory defined at the GUT scale down to low energies. Our approach is to run down all the Yukawa matrices from the GUT scale down through the heavy right-handed neutrino mass thesholds to low energy, replacing the neutrino Yukawa matrices by the dimension 5 neutrino mass operator at the lowest right-handed neutrino mass threshold. We have found that in the realistic cases considered, the atmospheric and solar neutrino mixing parameters receive radiative corrections of order 10% and 5%, respectively, while the ratios of the neutrino masses change by up about 50% in going from M_U to low energy. Importantly, more than 50% of the overall radiative corrections arises from running through the threshold region, even though it only accounts for two orders of magnitude in energy. Thus many of the existing analyses in the literature which ignore this threshold region could endanger a significant error.

We have considered a realistic class of models known as SRHND [8, 9], in which the contribution to the 23 block of the light effective Majorana matrix m_{LL} is dominated by a single right-handed neutrino. The small neutrino mass hierarchy $m_{\nu_2}/m_{\nu_3} \sim 0.1$

originates from the smallness of the 23 subdeterminant of m_{LL} (which is zero in the limit that a single right-handed neutrino is the only contribution). We have focussed on cases with two large mixing angles θ_{23} and θ_{12}, with the CHOOZ angle θ_{13} being small - the so-called bi-maximal mixing scenario. The couplings of the dominant right-hand neutrino controls the 23 and 13 mixing angles, and the subdominant right-handed neutrino couplings control the 12 angle. A $U(1)$ family symmetry is used to generate a controlled expansion of all the Yukawa couplings in powers of the Wolfenstein parameter λ, and with a suitable choice of $U(1)$ charges SRHND may be achieved with subdominant right-handed neutrino contributions being of the correct order of magnitude to generate the desired neutrino mixing angles and mass hierarchy.

The $U(1)$ charges also control the charged lepton Yukawa matrix, resulting in large contributions to the physical lepton mixing angles from the charged lepton sector. In general one would expect the two contributions to the 23 mixing angle (from the charged leptons and the neutrinos) not to cancel exactly due to order unity coefficients in the Yukawa matrices which are not predicted, and our numerical results include these effects. Similarly it would be surprising if the physical mixing angles turned out to be exactly maximal at the GUT scale. Therefore we have considered examples in which the 23 and 12 angles start out large but not maximal, and we have also assumed large $\tan \beta$, where the τ Yukawa coupling is large and the effect of radiative corrections is maximised. Although the effect of radiative corrections on the mixing angles is always $\leq 10\%$, showing that the models are quite stable, we have shown that the effects may play an important role in driving the initially large (but not maximal) mixing angle towards its maximal value. This is true both of the atmospheric mixing angle and the solar mixing angle, although in the latter case the effects are milder, which helps to explain why the atmospheric angle is larger than the solar angle. In principle, a different choice of parameters could have caused the neutrino angles to have grown smaller at low energies. However it is significant that

for the cases considered both mixing angles become magnified showing that the low energy approximate bi-maximal scenario could partly result from radiative corrections in SRHND models.

References

[1] H. Sobel, talk presented at the XIX International Conference on Neutrino Physics and Astrophysics, Sudbury, Canada, June 16-21, 2000.

[2] Y. Suzuki, talk presented at the XIX International Conference on Neutrino Physics and Astrophysics, Sudbury, Canada, June 16-21, 2000.

[3] L. Wolfenstein, Phys. Rev. **D17** (1978) 2369;
S. Mikheyev and A. Yu. Smirnov, Sov. J. Nucl. Phys. **42** (1985) 913.

[4] V.N. Gribov, B.M. Pontecorvo, *Phys. Lett.* **B 28** (1969) 493.

[5] J.N. Bahcall, P.I. Krastev, A.Yu. Smirnov, Phys. Rev.**D60** (1999) 093001, hep-ph/9905220.

[6] M. Gell-Mann, P. Ramond and R. Slansky in Sanibel Talk, CALT-68-709, Feb 1979, and in *Supergravity* (North Holland, Amsterdam 1979);
T. Yanagida in *Proc. of the Workshop on Unified Theory and Baryon Number of the Universe*, KEK, Japan, 1979;
R.N.Mohapatra and G.Senjanovic, Phys.Rev.Lett.**44** (1980) 912.

[7] J. Ellis, G.K. Leontaris, S. Lola, D.V. Nanopoulos, Eur. Phys. J. **C9** (1999) 389, hep-ph/9808251; S. Lola and G.Ross, Nucl. Phys. **B553** (1999) 81, hep-ph/9902283; G. Leontaris, S. Lola and G . Ross, Nucl. Phys. **B454** (1995) 25; H. Dreiner, G. Leontaris, S. Lola G. Ross and C. Scheich, Nucl. Phys. **B436** (1995) 461; K. S. Babu, C. N. Leung and J. Pantaleone, Phys. Lett. **B319** (1993) 191;

G. Altarelli and F. Feruglio, Phys. Lett. **B439** (1998) 112, hep-ph/9807353; G. Altarelli and F. Feruglio, JHEP 9811:021 (1998), hep-ph/9809596, G. Altarelli and F. Feruglio, Phys. Lett. **B451** 388 (1999), hep-ph/9812475; G. Altarelli and F. Feruglio, Phys.Rept. **320** 295 (1999), hep-ph/9905536; G. Altarelli, F. Feruglio, I. Masina, Phys.Lett. **B472** 382 (2000), hep-ph/9907532; R. Barbieri, P. Creminelli and A. Romanino, Nucl.Phys.**B559** 17 (1999), hep-ph/9903460; K.R.S. Balaji, Amol S. Dighe, R.N. Mohapatra, M.K. Parida, Phys.Rev.Lett.**84** (2000) 5034, hep-ph/0001310.

[8] S. F. King, Phys. Lett. **B439** (1998) 350, hep-ph/9806440; *ibid* ,Nucl. Phys. **B562** (1999) 57, hep-ph/9904210.

[9] S. F. King, Nucl. Phys. **B576** (2000) 85, hep-ph/9912492.

[10] J. Ellis and S. Lola, Phys.Lett.**B458** (1999) 310, hep-ph/9904279; N. Haba, Y. Matsui, N. Okamura,hep-ph/9911481; P. H. Chankowski, W. Krolikowski and S. Pokorski, Phys.Lett. **B473** 109 (2000), hep-ph/9910231.

[11] J. A. Casas, J. R. Espinosa, A. Ibarra and I. Navarro, Nucl. Phys. **B556** (1999) 3, hep-ph/9910420.

[12] Z. Maki, M. Nakagawa and S. Sakata, Prog. Theo. Phys. **28** (1962) 247.

[13] M. Apollonio *et al*, Phys.Lett. **B420** 397 (1998), hep-ex/9711002.

[14] C. D. Froggatt and H. B. Nielsen, Nucl. Phys. B147 (1979) 277.

[15] H. Fritzsch, Phys. Lett. 70B (1977) 436; B73 (1978) 317; J. Harvey, P. Ramond and D. Reiss, Phys. Lett. B92 (1980) 309; C. Wetterich, Nucl. Phys. B261 (1985) 461; P. Kaus and S. Meshkov, Mod. Phys. Lett. A3 (1988) 1251.

[16] L. Ibanez and G.G. Ross, Phys. Lett. B332 (1994) 100; P. Binetruy and P. Ramond, Phys. Lett. B350 (1995) 49, hep-ph/9412385.

[17] J. Elwood, N. Irges and P. Ramond, Phys. Rev. Lett. **81** (1998) 5064, hep-ph/9807228; N. Irges, S. Lavignac and P. Ramond, Phys. Rev. **D58** (1998) 035003, hep-ph/9802334.

[18] M. Green and J. Schwartz, Phys. Lett. B149 (1984) 117.

[19] L. Wolfenstein, Phys. Rev. Lett **51** (1983) 1945.